Met. Mater. Int., Vol. 21, No. 3 (2015), pp. 580~587
doi: 10.1007/s12540-015-4448-0

Assessment of Heat Transfer Through Mold Slag Film Considering Radiative Absorption Behavior of Mold Fluxes

Dae-Woo Yoon[1], Jung-Wook Cho[2,*], and Seon-Hyo Kim[1]

[1]Department of Materials Science and Engineering, Pohang University of Science and Technology, Pohang, 790-784, Republic of Korea
[2]Graduate Institute of Ferrous Technology (GIFT), Pohang University of Science and Technology, Pohang, 790-784, Republic of Korea

(received date: 28 September 2014 / accepted date: 14 November 2014)

Controlling the heat transfer rate from solidifying shell to copper mold is one of the important role of mold flux film during continuous casting of steels. It is highly desirable to regulate the thermal resistance of mold flux film not to exceed the critical quantity of mold heat transfer rate to prevent cast steel products from surface defects. In order to examine the effect of thermal radiation on the overall heat transfer rate through slag film in the continuous casting mold, the absorption coefficient has been investigated for various mold fluxes using a UV and an FT-IR spectrometer, followed by numerical calculations based on gray gas assumption. It is estimated that the heat transfer rate will decrease in 2-4% by addition of 3.2 mass% NiO into the conventional mold flux system with basicity (CaO/SiO_2) of 1.07. As the increase of absorption coefficients will not be harmful to any casting performances such as friction in a casting mold, it is highly recommended to enhance the thermal radiative absorption behavior of mold slag film by optimizing the chemistry of mold fluxes, especially in the wavelength range of 1 to 3 μm at which the emitted energy intensity from steel shell will be maximized.

Keywords: casting, mold flux, radiation, optical properties, NiO

1. INTRODUCTION

During the continuous casting of steel, controlling mold heat transfer rate is one of the most important functions of mold flux film infiltrated into the gap between copper mold and solidifying steel shell. As the occurrence of surface defects on continuously cast steel products is intensively accelerated by the excessive mold heat transfer rate especially during initial solidification of the molten steel in mold, the mold flux film should have enough thermal resistance to maintain optimum mold heat transfer rate. It is well known that the mold flux film consists of two layers: a molten glassy layer nearby the steel shell and another solid layer mixture of glass and crystalline. These layers provide the mold flux film with thermal resistances to the conductive and radiative heat transfers in the mold [1]. In addition, experimental studies showed that another thermal resistance caused by the air gap at mold/mold flux film interface played an important role in the heat transfer in the mold as shown in Fig. 1 [2,3]. Thus, understanding of thermal resistances arising from the molten slag layer, crystalline layer and the air gap is essential for the heat transfer analysis [1,4]. Many previous reports suggested that the mold heat transfer rate would be decreased by increasing crystallinity of mold slag film [3,5-7], which is attributed to the increase of interfacial thermal resistance [3,5] or the increase of extinction coefficients [8]. Therefore, highly basic mold fluxes [9] have been applied to the crack-sensitive steel grades to suppress the peak mold heat transfer rate near the meniscus. However, poor lubrication resulted from higher crystallinity in mold slag film may bring different kinds of surface defects [10] such as streak marks or a sticker breakout. In this context, it is highly desirable that the liquid glassy mold flux film layer would have sufficient amounts of thermal resistance, which can enable proper control of both the heat transfer and lubrication in a casting mold.

In general, the thermal radiation is regarded as a decisive mode of heat transfer through liquid glassy slag film. Several attempts [1,8,11] have been made with study on the absorption coefficient of mold fluxes, and the latter is a significant property for thermal radiation. Susa *et al.* [12,13] reported that absorption coefficient is known to be markedly dependent on the concentrations of transition metal oxides in mold slag systems. However, no systematic investigation has been carried out to

*Corresponding author: jungwook@postech.ac.kr

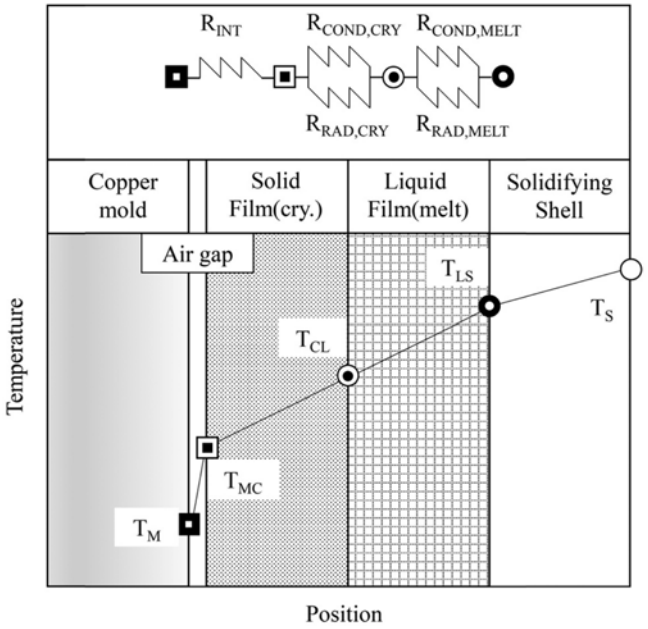

Fig. 1. Schematic of heat transfer through mold flux film.

understand the possibility of controlling the overall mold heat transfer rate by optimization of thermal radiation through liquid slag film. The aim of this study is, therefore, to attain comprehensive understanding of mold heat transfer through mold flux film considering the thermal radiation absorption into glassy phase for various commercial and modified mold flux system. The multi oxyflouride of CaO-SiO_2-Na_2O-Al_2O_3-F system has been investigated to understand the thermal radiation through commercial mold fluxes. Also, the modified mold flux system by addition of B_2O_3 or NiO has been investigated to clarify the effect of the slag structure or charge transfer on the thermal radiation behavior, respectively.

2. EXPERIMENTAL PROCEDURES

2.1. Sample preparation

Based on a survey of chemistry of the commercial mold fluxes for various steel grades, seven mold fluxes were designed for the investigation of thermal radiation as shown in Table 1. Mold fluxes containing B_2O_3 or NiO were manufactured based on B-mold flux. To prepare the sample for thermal radiative absorption, each mold flux was melted at 1573 K in a electric resistance furnace, and then quenched in a copper mold, annealed to remove thermal stress for glassy specimens at 673 K for 1 h, cut and polished to make a thin disc of 13 mm in diameter and 8-25 mm in thickness.

2.2. Definition of absorption coefficient

The absorption behavior of the mold fluxes was investigated using a Fourier transformation infrared spectroscopy from 1,500 to 4,000 cm^{-1}. Also, 4,000-20,000 cm^{-1} spectral range were analyzed by using an ultraviolet-spectrometer. The spectral resolution was 2 cm^{-1}. During the spectrometric observation, radiation intensity, I_λ, irradiates on a specimen of thickness l. As the radiation goes through the specimen layer, its intensity is reduced by extinction and reflection. In this study, the reflectivity of both the glassy and crystalline mold flux films will be ignored based on the previous investigation by one of the present authors [1] from whom the reflectivity for the commercial mold fluxes have been measured to be 1 to 3%, regardless of the degree of crystallinity. Detailed explanation to evaluate reflectivity of mold fluxes have been reported by Cho *et al.* [1].

The extinction coefficient consists of two parts, an absorption coefficient and a scattering coefficient. For glassy specimen, a scattering factor could be neglected compare to the extinction coefficient.

$$\frac{I_\lambda(l)}{I_\lambda(0)} = \exp(-\alpha_\lambda l) \tag{1}$$

Equation (1), known as Lambert-Beer's law shows that the intensity of thermal radiation emitted from the steel shell will decrease exponentially along a path through an absorbing medium, i.e., the mold flux film [14]. Extinction coefficient for crystalline mold flux is determined to be 10,000-12,000 m^{-1} for all mold fluxes on the basis of Cho *et al.*'s observations [1] in the range of 2.0-5.0 μm.

3. RESULTS AND DISCUSSION

3.1. Absorption coefficient and optical properties

Most of the radiative heat transfer takes place in the wavelength range of 1 to 6 μm by using Planck's law as shown in Fig. 2 on the assumption of blackbody radiation from steel shell. As the energy intensity in the range of 1.0-3.0 μm accounts

Table 1. Chemical composition of mold fluxes (mass%)

Mold flux	SiO_2	CaO	MgO	Al_2O_3	Fe_2O_3	Na_2O	F	Li_2O	B_2O_3	NiO	Basicity
A	45.8	34.3	0.7	4.8	0.7	7.2	6.5	-	-	-	0.75
B	41.1	38.5	0.8	5	0.7	7.3	6.6	-	-	-	0.94
B-1	39.3	37.5	0.7	5.1	0.9	7.5	7.2	1.8	-	-	0.95
B-2	35.6	35.8	0.9	4.2	0.3	6.0	5.5	-	11.7	-	1.0
C	36.7	41.7	0.8	5.3	0.6	7.5	7.4	-	-	-	1.14
D	33.4	44.8	0.8	5.4	0.5	7.6	7.5	-	-	-	1.34
N	36.5	39.0	0.8	5.4	0.8	7.2	7.1	-	-	3.2	1.07

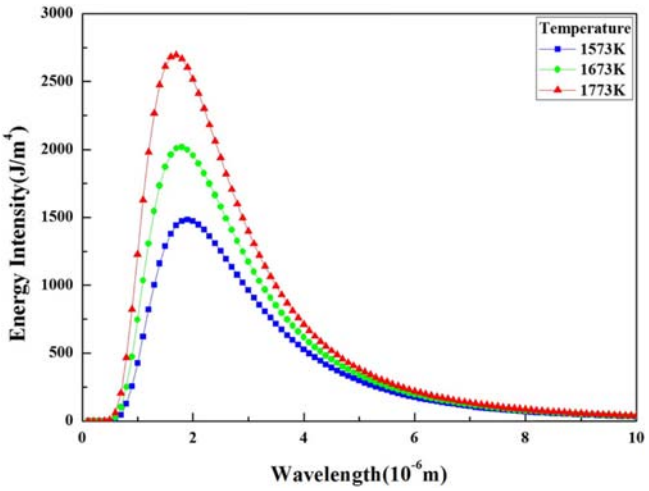

Fig. 2. Wavelength range of radiative heat flux: Plank's law on the assumption of black body.

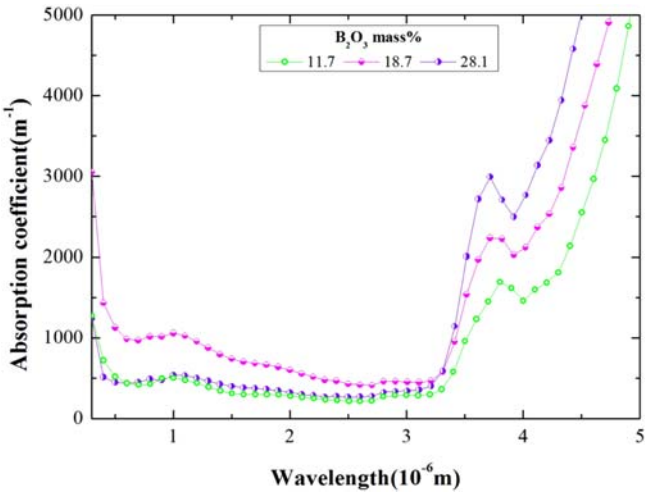

Fig. 4. Absorption coefficient of (100-x)(B-mold flux)·xB_2O_3(mass%) mold slag as function of wavelength.

for nearly 62% of total emitted energy, particular attention should be paid to the absorption coefficient of mold fluxes in near infrared range to understand thermal radiation in continuous casting mold. According to the investigation by Kusabiraki and Shiraishi [15-17], the absorption coefficient at 673 K of solidified glassy specimen would not lead to much error when calculating radiative heat transfer through liquid flux layer. Therefore, the absorption coefficients for all the studied mold fluxes were measured at room temperature as shown in Fig. 3. Absorption coefficients of glassy mold fluxes in the infrared range are largely below 1,000 m^{-1}. All of the glassy fluxes investigated except for B-2 show sharp increase of absorption coefficient beyond wavelength of 4.5 μm due to the stretching vibration of Si-O bonds. This result agrees with the investigation by Cho *et al.* [1] who reported nearly transparent range below wavelength of 4.5 μm for various mold slag systems.

The effect of B_2O_3 addition on the absorption coefficient of B-mold flux based slag is shown in Fig. 4. The increase of absorption coefficient in the 3.78-4.06 μm range by addition of boron oxide is believed to arise from the ring stretch of cyclic meta-borate ion [18]. However, addition of borate oxide into mold fluxes will not make a significant change in the thermal radiation through mold flux film because this range is far away from the peak intensity of emitted thermal radiation from steel as shown in Fig. 2. However, the effect of NiO addition on the absorption coefficient of slag system is markedly different as shown in Fig. 5. There is a distinct increment in the range of 0.5-2.7 μm with increasing NiO concentration. The spectra includes three absorption peaks at 0.45, 0.95, and 1.85 μm which are in good accordance with the d-orbital transitions, $^3A_{2g}(F)\rightarrow{}^3T_{1g}(P)$, $^3A_{2g}(F)\rightarrow{}^3T_{1g}(F)$, $^3A_{2g}(F)\rightarrow{}^3T_{2g}(F)$, for nickel ion in octahedral symmetry on the basis of the report for alkali tetra-borate glasses containing NiO [19]. Out of

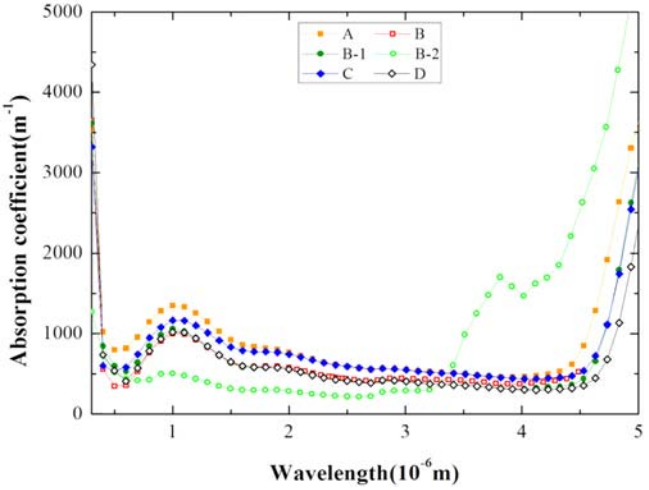

Fig. 3. Absorption coefficient of commercial mold fluxes as function of wavelength.

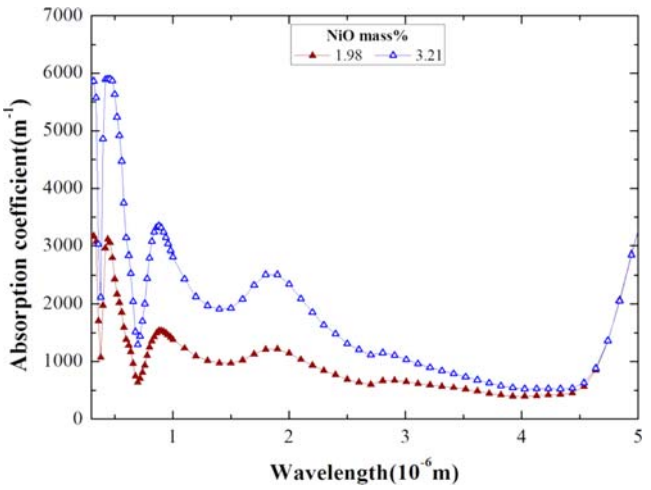

Fig. 5. Absorption coefficient of (100-x)(B-mold flux)·xNiO(mass%) mold slag as function of wavelength.

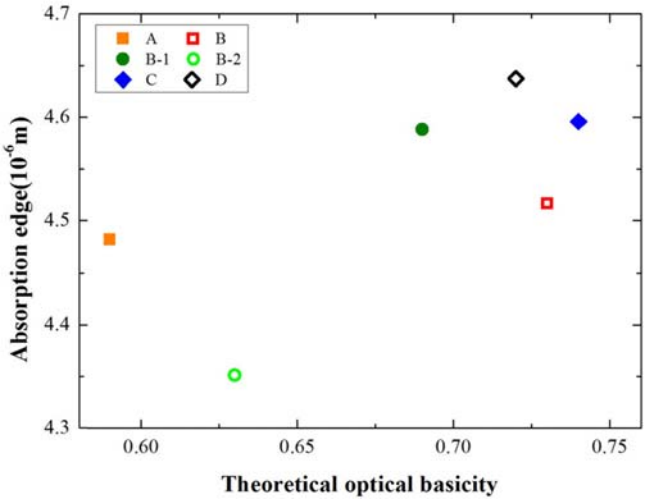

Fig. 6. Shift of absorption edge for commercial mold slags as function of optical basicity.

various investigated mold fluxes, those mold fluxes containing nickel oxide show appropriate thermal radiation absorption in the range of the near infrared which is capable of regulating radiative heat flux density through mold slag film. In Figures 3 to 5, one can define the absorption edge where the absorption coefficients increase drastically. The absorption edge of investigated mold fluxes has been determined by differentiation of each absorption plots. As shown in Fig. 6, the absorption edge tends to shift to higher wavelengths with higher basicity due to Si-O bond stretching, which is in agreement with the finding by Hayashi *et al.* [20] who showed that the absorption edge shifts to higher wavelengths with increasing the electron donor power of oxygen ions. The variation of absorption coefficients could be influenced by considerable shift of absorption edges to the vicinity of peak emission intensity as shown in Fig. 2, which is not the case for the investigated mold fluxes in this study.

3.2. Calculation of overall mold heat transfer rate near meniscus

To evaluate the effect of investigated thermal radiation absorption on heat transfer through mold flux film in the vicinity of meniscus, total heat transfer rate has been calculated based on following assumptions. In calculation, the mold flux film was regarded as a combination of solid and liquid layers in parallel as shown in Fig. 1. Also, the overall heat transfer was assumed to be steady state and one dimensional through the whole mold flux film. When there is no interference between the radiation and conduction, total heat flux for the liquid layer and crystallized layer can be expressed as

$$q_{TOT} = q_{COND,MELT} + q_{RAD,MELT} \quad (2)$$

$$q_{TOT} = q_{COND,CRY} + q_{RAD,CRY} \quad (3)$$

Table 2. Reference processing conditions and physical properties

Position	30 mm below the meniscus
V_c (m/min)	1.0
d_{shell} (mm)	$15/(0.03/V_c)^{0.5}$ [21]
R_{INT} (m^2·K/W)	$0.29392 \cdot d_{shell} + 0.00035151$
T_M (K)	593
T_S (K)	1780
T_{CRY} (K)	1313
K_{COND} (W/m·K)	31.1 (steel shell)[22] 1.73 (crystalline mold flux)[1] 1.33 (liquid mold flux)[1]
ε	0.78 (steel shell)[23] 0.4 (copper mold)[23]
n	1.6[20]

where,

$$q_{COND,MELT} = k_{COND,MELT}(T_{LS} - T_{CL})/d_{MELT} \quad (4)$$

$$q_{COND,CRY} = k_{COND,CRY}(T_{CL} - T_{MC})/d_{CRY} \quad (5)$$

In eqs. (2) through (5), (T_{CL}-T_{MC}) and (T_{LS}-T_{CL}) is temperature gradient in crystalline layer and molten layer, respectively, as shown in Fig. 1. Thermal conduction could be calculated by using temperature gradient and thermal conductivity with film thickness of each phase. The reference processing condition and physical properties used for the calculation are given in Table 2 [1,20-23]. In order to demonstrate sharp temperature gradient between solidified steel shell and copper mold, gray gas approximation can be applied. In this approach, the absorption coefficient of the medium, the gray gas, is presumed to be independent on both wavelength and temperature [1]. Thermal radiation for the medium between two infinite parallel plate at temperature T_1 and T_2 can be expressed as

$$q_{RAD} = A \cdot (T_1^4 - T_2^4) \quad (6)$$

$$A = n^2\sigma/(0.75\alpha l + 1/\varepsilon_1 + 1/\varepsilon_2 - 1) \quad (7)$$

In eq. (7), one can define a representative absorption coefficient in consideration of spectral intensity from the plate. In this study, the averaged absorption coefficient was given as following, which is suggested by Ohta *et al.* [24]

$$\alpha = -\frac{\partial[\log Tr(l)]}{\partial l} \quad (8)$$

$$Tr(l) = \int \frac{e_{\lambda b}\exp(-\alpha_\lambda l)}{e_b} d\lambda \quad (9)$$

$$e_{\lambda b} = 2\pi h c_0^2/\{\lambda^5[\exp(hc_o/k\lambda T) - 1]\} \quad (10)$$

where, $Tr(l)$ is transmittance through medium thickness, l, in the range of wavelength measured by FT-IR and UV-spectrometer in this study.

One can calculate radiative thermal conductivity of molten flux film layer by using gray gas assumption as

$$q_{RAD,MELT} = k_{RAD,MELT}(T_{LS} - T_{CL})/d_{MELT} \quad (11)$$

$$k_{RAD,MELT} = A(T_{LS}^4 - T_{CL}^4)d_{MELT}/(T_{LS} - T_{CL}) \quad (12)$$

$$A = n^2\sigma/(0.75\alpha l_{MELT} + 1/\varepsilon_{MELT} + 1/\varepsilon_{CRY} - 1) \quad (13)$$

which should be similar to crystalline layer as

$$q_{RAD,CRY} = k_{RAD,CRY}(T_{CL} - T_{MC})/d_{CRY} \quad (14)$$

$$k_{RAD,CRY} = A(T_{CL}^4 - T_{MC}^4)d_{CRY}/(T_{CL} - T_{MC}) \quad (15)$$

$$A = n^2\sigma/(0.75\alpha l_{CRY} + 1/\varepsilon_{MOLD} + 1/\varepsilon_{STEEL} - 1) \quad (16)$$

Using Eqs. (11)-(16), the total heat transfer rate in Eqs. (2) and (3) can be obtained. The overall numerical calculation has been conducted by following steps as shown in Fig. 7: i) calculations of total interfacial thermal resistance and total heat flux by using thermal conductivities of each phase (crystalline, liquid mold flux) and thickness of mold flux film, ii) computing intermediate temperature of interfaces between steel shell/liquid flux film layer, liquid film/solid film and solid film/copper mold with effective thermal conductivities of each phase, iii) obtaining k_{RAD} using converged thickness, temperature of each phase and gray gas assumption, iv) defining total heat flux by using converged k_{RAD}. All the numerical calculation mentioned above have been carried out using FORTRAN.

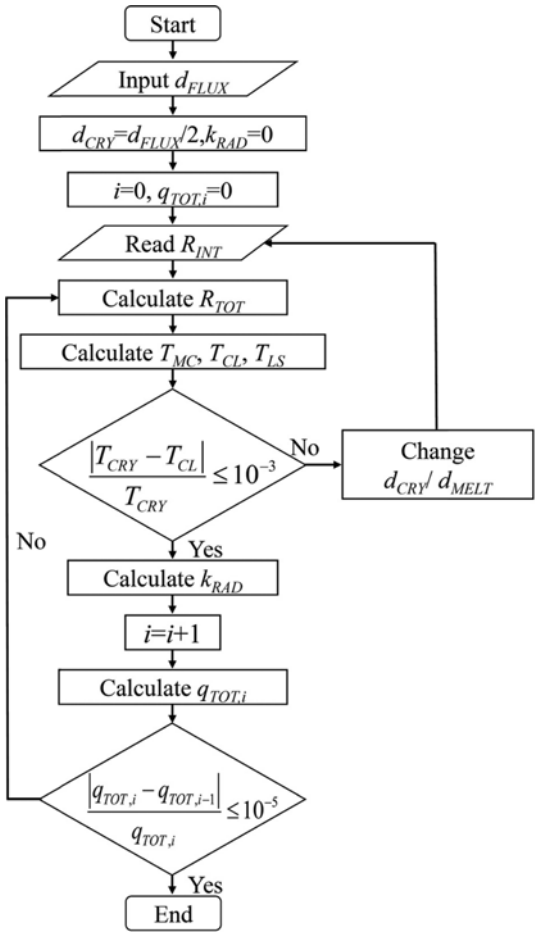

Fig. 7. Flow chart for calculating heat transfer rate.

3.3. Effect of absorption coefficients and other casting conditions on overall mold heat transfer rate

Beside the absorption coefficient measured for each mold flux, other casting conditions such as conductive thermal conductivity, interfacial thermal resistance, mold temperature and crystallization temperature are considered as variables. Generally, overall mold heat transfer rate across mold flux film decreases exponentially with increasing flux film thickness as shown in Fig. 8. Two kinds of attempts have been made to obtain conductive thermal conductivity: laser flash method and hot wire method. As the report show deviations with the different measuring methods, both thermal conductivities from laser flash (k_{COND}=1.73(W/m·K)) [1] and hot wire (k_{COND} =0.8 (W/m·K)) [25] methods have been considered. In Fig. 8(a), calculation considering thermal conductivity from laser flash method shows *ca.* 9-11% larger mold heat transfer rate than that from hot wire method in a fixed flux thickness at 2 mm. Cho *et al.* [1] reported interfacial thermal resistance for the commercial mold fluxes with similar basicity as this study.

$$R_{INT}(10^{-4}m^2K/W) = 2.94d_{CRY}(\text{mm}) + 3.52\,,$$

$$\text{for } 0.3\text{mm} \le d_{CRY} \le 1.0\text{mm} \quad (17)$$

This interfacial thermal resistance is attributed to the air gap at the interface between copper mold and mold flux film in contact [26]. Decreasing interfacial thermal resistance causes the reduction of total heat flux in the amount of *ca.* 17-18% with casting conditions and mold fluxes at a d_{FLUX} of 2 mm as shown in Fig. 8(b). The effect of mold temperature on total heat flux is also studied, in 473K and 773K, respectively. The heat transfer rate decreases markedly, *ca.* 13-15% of q_{TOT} at a d_{FLUX} of 2 mm as shown in Fig. 8(c), by increasing mold surface temperature due to a decline of temperature gradient between mold and shell. In order to evaluate the effect of crystallization temperature, calculation has been carried out for two conditions, 1113 K and 1313 K as shown in Fig. 8(d). It is confirmed that increasing of crystallization temperature reduces *ca.* 10-11% of thermal radiation at a d_{FLUX} of 2 mm by increasing degree of crystallinity. This is in a good agreement with the investigation by Hanao *et al.* [27] who reported the reduction of about 10-15% of local heat flux by increasing the crystallization temperature of the mold flux from 1307 K to 1509 K.

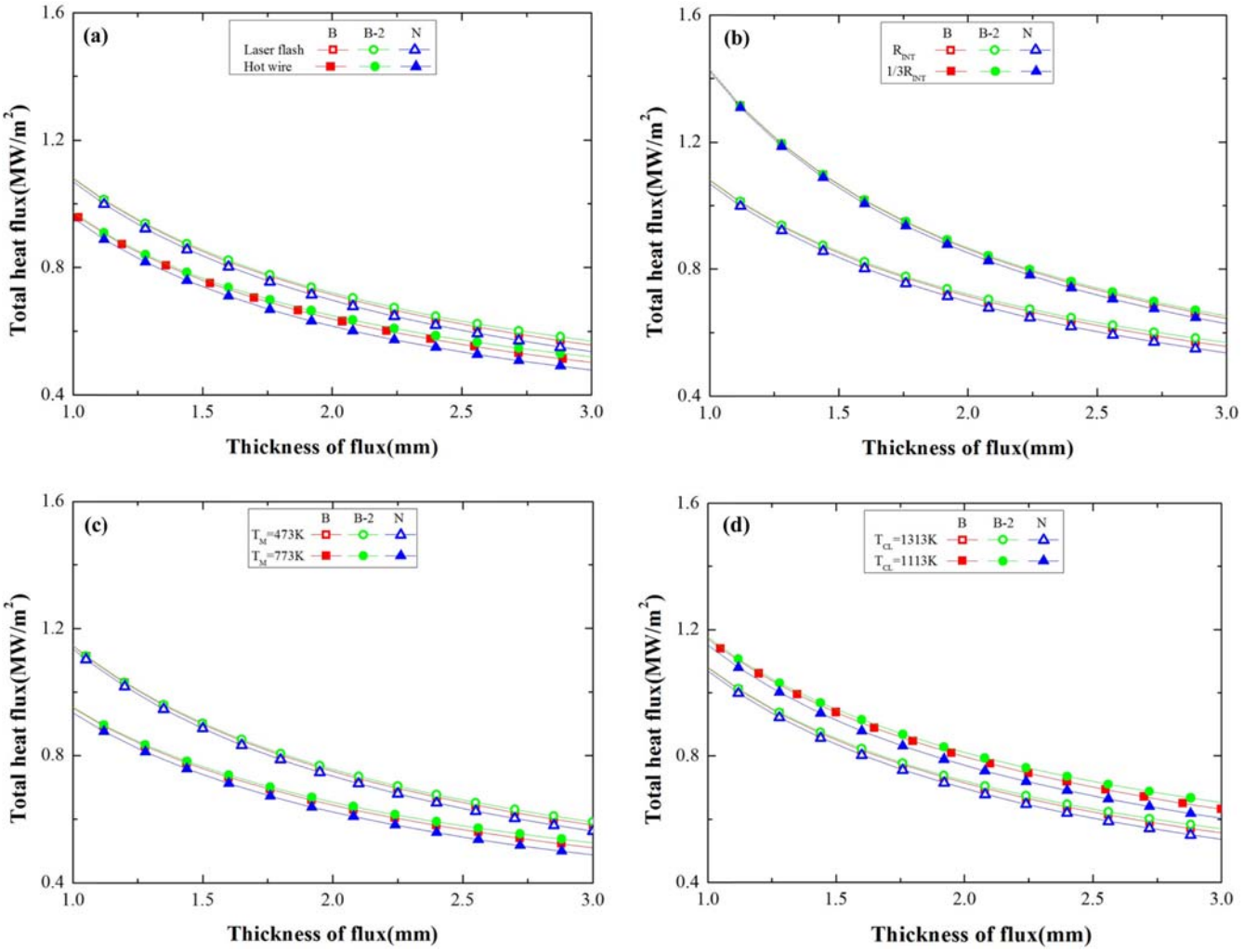

Fig. 8. Heat transfer rate calculated based on absorption coefficient and other casting operation conditions. (a) Conductive thermal conductivity, (b) Interfacial thermal resistance, (c) Copper mold surface temperature, and (d) crystallization temperature of mold flux.

Comparing with other examined physical properties, absorption coefficients show smaller effects on overall heat transfer rate. However, mold fluxes which contain transition metal oxide have a meaningful impact on the radiative heat flux density as shown in Fig. 8. By addition of 3.2 mass% NiO into conventional mold flux system, the heat transfer rate decreases *ca.* 2-4% at a d_{FLUX} of 2 mm. As nickel oxide dissolved in the melt, it is assumed that absorption intensity increase over the wavelength range of 0.5-5 μm. It would reduce total heat flux due to decrease radiative heat transfer by increasing absorption coefficient. On the contrary, Susa *et al.* [13,28] reported that the thermal radiation through mold flux will be enhanced by addition of transition metal oxides such as Fe_2O_3. It is believed that the different results between Susa *et al.* and the present study mainly arises from the different thermal properties applied to calculation, i.e. absorptivity of liquid film and reflectivity of solid film. Regarding the thermal radiation through liquid film, Susa *et al.* assumed very low absorption coefficient of zero [28] or 200 m^{-1} [13], which are much smaller than that of the NiO added mold flux as shown in Fig. 5. Adding to this, Susa *et al.* applied much larger reflectivity at the crystalline solid slag film surface, *ca.* 0.8 for the mold flux system without Fe_2O_3 and ca. 0.3~0.6 for those containing 0.25~2% Fe_2O_3, while reflection on solid film has been ignored in this study, as previous mentioned in chapter 2.2. Even though there is uncertainty about thermal properties of commercial mold flux film, it is worthy to note that the increase of absorption coefficients will not bring any detrimental effects on friction in a casting mold while any other countermeasures to enhance the degree of crystallinity will significantly disturb lubrication. Therefore, it is highly desirable to optimize the effect of transition metal oxide such as NiO which has a significant influence on the increase of absorption coefficients in near infrared region by a small amount of addition.

4. CONCLUSIONS

Radiative heat flux through slag film in continuous casting mold has been investigated for various mold fluxes. For calculation of radiative heat transfer rate, the absorption coefficient was measured in the wavelength range of 0.3-5 μm using a UV and an FT-IR spectrometry, followed by numerical analysis. The results are summarized as follows:

(1) Among various investigated mold fluxes, those containing nickel oxide show distinct increment of absorption coefficient in the range of 0.5-2.7 μm, which is coincident with the peak emission from solid steel shell during continuous casting of steel. By addition of 3.2 mass% NiO into the conventional mold flux system, the total mold heat transfer rate will decrease *ca.* 2-4%.

(2) The absorption edge due to stretching of Si-OH bonds increases with decreasing the mold flux basicity. Also, sharp increase in absorption coefficient is found in the range of 3.78-4.06 μm for mold fluxes containing B_2O_3 due to the ring stretch of cyclic meta-borate ion. However, the effect of these behaviors on mold heat transfer rate are negligible.

(3) The mold heat transfer rate will decrease by *ca.* 9-18% when the crystallinity of slag film will increase by changing casting conditions such as thermal conductivity, interfacial thermal resistance, mold temperature and crystallization temperature of mold flux. However, lubrication between the casting mold and steel shell may be deteriorated due to these changes.

NOMENCLATURES

c_o : propagation speed of electromagnetic radiation in vacuum (2.9979×10^8m/s)
d : thickness of each layer (mm)
d_{shell} : solidifying steel shell thickness (mm)
e : emissive power (W/m^2)
h : Plank's constant (6.6238×10^{-34}J·s)
I : radiative intensity (W/m^2·sr)
$I(0)$: radiative intensity impinging the layer (W/m^2·sr)
$I(l)$: transmitted infrared intensity (W/m^2·sr)
k : thermal conductivity (W/m·K)
l : specimen thickness (m)
n : refractive index
q : heat flux (W/m^2)
q_{TOT} : sum of heat flux of radiation and conduction (W/m^2)
R : thermal resistance (m^2·K/W)
R_{TOT} : sum of thermal resistance of air gap and mold flux film (m^2·K/W)
V : velocity (m/min)
T : temperature (K)
T_{CRY} : crystallization temperature of mold flux (K)
α : absorption coefficient (m^{-1})
ε : emissivity
σ : Stephan-Boltzmann constant (5.67×10^{-8}W/m^{2}K^4)
λ : wavelength (μm)

Subscripts

b : blackbody
C : continuous casting
CL : interface of crystalline mold flux film/molten layer of mold flux film
COND : conduction
CRY : crystalline layer of mold flux film
FLUX : mold flux film
INT : interface of copper mold/mold flux film
MELT : molten layer of mold flux
LS : interface of molten layer of mold flux/steel shell
M : copper mold surface
MOLD : copper mold
MC : interface of copper mold/crystalline layer of mold flux film
RAD : radiation
S : solidus line
λ : wavelength
λ_b : spectral distribution of blackbody

REFERENCES

1. J. W. Cho, T. Emi, H. Shibata, and M. Suzuki, *ISIJ Int*. **38**, 268 (1998).
2. S. Ohmiya, K. H. Tacke, and K. Schwerdtfeger, *Ironmak. Steelmak.* **10**, 24 (1983).
3. J. W. Cho, T. Emi, H. Shibata, and M. Suzuki, *ISIJ Int*. **38**, 440 (1998).
4. W. Wang, L. Zhou, and G. Kezhuan, *Met. Mater. Int.* **16**, 913 (2010).
5. J. W. Cho, T. Emi, H. Shibata, and M. Suzuki, *ISIJ Int*. **38**, 843 (1998).
6. E. Y. Ko, J. Choi, J. Y. Park, and I. Shon, *Met. Mater. Int.* **20**, 141 (2014).
7. J. Y. Park, E. Y. Ko, J. Choi, and I. Shon, *Met. Mater. Int.* **20**, 1103 (2014).
8. J. Diao, B. Xie, J. Xiao, and C. Ji, *ISIJ Int.* **49**, 1710 (2009).
9. J. W. Cho and H. Shibata, *J. Non-Cryst. Solids*, **282**, 110 (2001).
10. J. W. Cho, K. Blazek, M. Frazee, H. B. Yin, J. H. Park, and S.W. Moon, *ISIJ Int*. **53**, 62 (2013).
11. W. Wang, K. Gu, L. Zhou, F. Ma, I. Sohn, D. J. Min, H. Matsuura, and F. Tsukihashi, *ISIJ Int.* **51**, 1838 (2011).
12. M. Susa, K. Nagata, and K. C. Mills, *Ironmak. Steelmak.* **20**, 372 (1993).
13. M. Susa, A. Kushimoto, H. Toyota, M. Hayashi, R. Endo, and Y. Kobayashi, *ISIJ Int.* **49**, 1722 (2009).
14. R. Siegel and J. R. Howell, *Thermal Radiation Heat Transfer*, *2nd ed*., pp.412-447, Hemisphere Pub. Corp., Washington (1981).
15. K. Kusabiraki and Y. Shiraishi, *J. Jpn. Inst. Met.* **45**, 250 (1981).

16. K. Kusabiraki and Y. Shiraishi, *J. Jpn. Inst. Met.* **45**, 888 (1981).
17. K. Kusabiraki and Y. Shiraishi, *J. Jpn. Inst. Met.* **45**, 259 (1981).
18. I. C. Hisatsune and N. H. Suarez, *Inorg. Chem.* **3**, 171 (1964).
19. J. S. Berkes and W. B. White, *Phys. Chem. Glasses*, **7**, 191 (1966).
20. M. Hayashi, M. Susa, T. Oki, and K. Nagata, *ISIJ Int.* **37**, 126 (1997).
21. T. Mizoguchi, S. Ogibayashi, and T. Kajitani, *Tetsu-to-Hagane* **81**, 971 (1995).
22. K. Kobayashi, *Thermophysical Properties Handbook*, p.23, Yokendo, Tokyo (1990).
23. Y. Kawai and Y. Shiraishi, *Handbook of Physico-chemical Properties at High Temperature*, p.241, ISIJ, Tokyo (1988).
24. H. Ohta, M. Masuda, K. Watanabe, K. Nakajima, H. Shibata, and Y. Yaseda, *Tetsu-to-Hagane* **80**, 463 (1994).
25. Y. Kang and K. Morita, *ISIJ Int*. **46**, 420 (2006).
26. S. Bagha, N. C. Machingawuta, and P. Grieveson, *Proc. 3rd Int. Conf. on Molten Slags, Fluxes and Salts*, p.235, ISS, Glasgow (1988).
27. M. Hanao, M. Kawamoto, and A. Yamanaka, *ISIJ Int.* **52**, 1310 (2012).
28. M. Susa, A. Kushimoto, R. Endo, and Y. Kobayashi, *ISIJ Int.* **51**, 1587 (2011).